ACTA METALLURGICA SLOVACA
2023, VOL. 29, NO. 3, 167-176

TECHNICAL PAPER

THERMAL CHARACTERIZATION BY DILATOMETRY TESTS OF A FERRITIC-BAINITIC STEEL FOR AUTOMOTIVE APPLICATION

Matías Ezequiel Ramírez[1], *Elena Brandaleze*[1*]

[1] *Processes Technology Research Group, Metallurgy Department, Development and Technology of Materials Centre, National Technological University – San Nicolás Regional Faculty, Colón 332, San Nicolás, Argentina.*

*Corresponding author: ebrandaleze@frsn.utn.edu.ar, tel.: +54 9 336 4420830, San Nicolás Regional Faculty / National Technological University, 2900, San Nicolás, Argentina.

Received: 29.05.2023
Accepted: 20.08.2023

ABSTRACT

The main objective of this article is to deep the knowledge of the thermal behavior of ferrite-bainite (FB) steel in correlation with the structural aspects that justify the mechanical properties. Samples of a DP-590 steel were tested by dilatometry considering a heating rate of 0.17 °C/s, up to a temperature of 1150 °C and different cooling rates between 0.03 °C/s to 100 °C/s, in air atmosphere. The results of the thermal behaviour were correlated with a microstructural study using optical microscopy in order to establish the final proportion of ferrite and bainite that is achieved at each cooling rate considered. As the cooling rate increases, the diffusion processes are limited so that hard second phases are obtained. In this steel, the presence of bainite was corroborated. The mechanical strength evolution associated with the cooling rate was determined through microhardness measurements. On this base, the steel's continuous CCT curves was built.

Keywords: steel; biphasic; dilatometry; microstructure; thermodynamic simulation

INTRODUCTION

Currently, the automotive manufacturing the industry is in the forefront of research activities for two main reasons: a) improve passenger safety and b) decrease the fuel consume in order to minimize the amount of GEI emissions [1, 2]. With the interest of achieve these purposes, different types of alloys, are considered.

The HSLA steels constitute relevant alloys for structural applications in the automotive parts production [1]. However, aligned with this purpose, it is necessary to reduce the steel sheet thickness without any effect on the mechanical strength. In this sense, there are different high-strength steels that could be used in automotive productions. In this sense, there are different high-strength steels that could be used in automotive productions. According with the application criteria mentioned in [2], some of convenient steels to select are: a) Dual-Phase (DP), with a ferrite-martensite structure, b) High hole expansion (HHE), that present a ferrite-bainite structure, c) Stretch flangeable (SF), d) Transformation induced plasticity (TRIP), e) Complex phase (CP), f) Fully martensitic (MS), g) Boron heat treatable steels, among others. The SF or HHE steels, also are biphasic with a ferritic-bainitic structure and are characterized by their aptitude to stretch or high hole expansion, respectively. However, it is relevant to mentioned that in the automotive industry these materials are distinguished simply as ferrite-bainite steels. These steels have a higher resistance to edge cracking compared to conventional DP (ferrite/martensite) steels and precipitation hardened steels, making them well suited in applications where flanged holes are required. For this reason, they are used for chassis and suspension parts, especially control arms [2].

The industrial production of them are as hot-rolled products and generally with thicknesses ≥ 2.0 mm. Hot forming of these type of steels constitutes a complex forming and tempering operation. Firstly, a full austenizing process is carried out, heating up at temperatures over the austenitic (γ) temperature transformation and maintained until fully homogeneous microstructure is achieved. Then the steel sheet is cooled down rapidly to obtain the biphasic (ferrite-bainite) microstructure. The thermomechanical evolution results in a steel with the required properties [1]. There are different process variants, however, the final microstructure as well as the mechanical properties of the part can be controlled very effectively depending on the holding temperature and the controlled cooling process. To obtain the optimum steel product, it is necessary to dispose a deep knowledge on the thermal evolution impact on the steel, in relation with microstructure and the transformation temperatures.

The material selected for this study is a biphasic ferrite-bainite steel. The final microstructure required is a combination of ductile ferrite and hard bainite. These steels are appropriated for automobile parts that demand the maximum amount of energy absorption during a crash event or to be used in auto parts which requires good stretch or hole expansion resistance. On this base, the cooling rate becomes a very important variable that allows to control ferrite and bainite amount in the final structure of the material. Therefore, the cooling rate controls the kinetic of $\gamma \rightarrow \alpha$ solid state phase transformation, the final microstructure, and the mechanical properties of the steel sheet.

Dilatometry tests were extensively used to increase the knowledge on the thermal process impact on the steel microstructure and were considered as an important tool for many researchers [3-8]. In this study, dilatometry tests provided information of the phase transformation temperatures during heating and under different cooling rate conditions of the steel. In addition, the tests allowed to understand the mechanisms and driving

force of the nucleation and growth of the phases generated, during the industrial thermomechanical processing [4]. These phenomena are influenced by crystalline structure and lattice parameters changes. Microstructural changes were detected and registered by the dilatometer, through the macroscopically volume changes in relation with temperature variation of the sample. The $\gamma \rightarrow \alpha$ phase transformation temperatures of the steel were precisely determined applying the methodology reported in [5]. It was also considered the appropriate methodology to determine the stability of each solid phase formed in the ferrite-bainite steel, during a continuous cooling. Based on these results, in this paper the continuous cooling transformation diagram of the DP steel (considering all the phases transformations involved) is presented. The study considered several cooling rates (between 0.03 and 100 °C/s). The methodology is in complete agreement with [6, 7]. The microstructure of all the samples were characterized and the results of present phases obtained, were correlated with a thermodynamic simulation applying the software FactSage 8.1 [8]. In this case, the cooling of the ferrite-bainite steel was simulated in the range between 400 °C to 1200 °C, at equilibrium conditions. The software also provides information related to the C diffusion process in the austenite and the other elements present in the steel composition, during cooling.

The microstructural study was carried out by light microscopy and the present microconstituents were identified and quantified on each sample in order to predict the mechanical behaviour of the selected steel. Furthermore, Vickers microhardness (H_V) measurements were carried out to complete the knowledge of the mechanical behaviour impact of each cooling condition applied.

According to [9], the cementite associated with bainite is different respect that found in pearlite, because of the different content of substitutional solutes in the matrix from which it grew. It is relevant to consider that upper bainite begins with the nucleation and growth of ferrite with the paraequilibrium carbon concentration, promoting the carbon enrichment of the residual austenite. Bainite grows constituting clusters of ferritic plates usually denominated sheaves with a low misorientation angle between them. Lower bainite consists in non-lamellar ferrite aggregates with two types of carbides: a finer dispersion with a plate-like morphology (observed inside the ferrite) and precipitates particles with a single crystallographic variant within the ferritic plate. Davenport and Bain [9] studied the mentioned transformations using both metallography and dilatometry. However, to increase the understanding of the thermal evolution it is necessary to correlate the information with a continuous cooling curve of the steel. Some studies carried out by Wever, on the bainitic structure formation, shows that bainitic transformation presents an incubation period, so it is possible to be assumed that occurs through a nucleation and growth process. In this sense, different researcher's opinions and models are discussed on bainitic transformation in the steel structure [9]. During the growth of bainitic ferrite there is not long-range redistribution of substitutional solutes and in consequence the ratio between iron and substitutional atoms remains constant. This phenomenon is explained because the transformation presents a displacive character.

The ferrite-bainite steel selected contains Nb and Ti microalloyed elements. Many failures of this type of steels could be caused by early carbides formation in the steel. It is known that the carbides particles generated in the upper bainite and low bainite are different [9]. For this reason, the evolution of the precipitates associated with temperature constitutes a relevant information to predict the material behaviour. The carbides precipitation in the bainite decrease the carbon content of the residual austenite. When carbide precipitation occurs in the austenite grain boundaries, they can affect the final material mechanical properties. It is important to mention that the main effect of carbon on the strength of this type of steel is through carbide precipitation. In this sense, the predictions of the precipitation phenomena obtained by Fact Sage at equilibrium conditions, contributed to understand the experimental results obtained and to predict the steel mechanical behaviour. All the information obtained was correlated with hot rolling industrial parameters and contributed with knowledge in order to adjust process operation conditions.

MATERIAL AND METHODS

The material selected for this study is a biphasic steel (ferritic-bainitic), hot rolled. This steel is characterized by a good combination of mechanical properties such as high strength and ductility. The chemical composition is showed in **Table 1**. The material was designated by the supplier as DP-590 steel due to the ultimate tensile strength value of 590 MPa. The steel sheet dimensions are: 1,295 mm of width, 500 mm of length and 3.29 mm of thickness. This thickness corresponds to the steel sheet hot-rolled.

Table 1 DP-590 steel chemical composition (wt. %)

C	Mn	P	S	Si	Cr	Ni	Al	Nb	Ti
0.12	1.25	0.01	0.01	0.12	0.02	0.03	0.06	0.05	0.009

The thermal characterization of the steel was carried out applying dilatometry tests. Twenty samples with a dimension of 3 mm × 3 mm × 10 mm, were tested. The essays were performed using two dilatometers: a) a THETA DILATRONICS II instrument for cooling rates between 0.03 °C/s and 10 °C/s from DEYTEMA Centre of UTN-FRSN, Argentina and b) a BAHR 805D instrument for cooling rates between 0.45 °C/s and 100 °C/s from CENIM Centre, of Spain. In all the cases, samples were heated at 2 °C/s up to 1,150 °C considering a holding time of 330 s to achieve the homogenous austenization. Finally, different cooling rates between 0.03 °C/s and 100 °C/s were applied. All the tests were performed in air atmosphere.

The dilatometric curves of all samples were plotted, the phase transformation temperatures and all critical points of the steel, were determined. On the base of these results, the cooling rates curves (temperature vs time curves) were constructed, to obtain the continuous cooling diagram of the DP-590 steel. To complete the knowledge of the steel evolution with temperature, a thermodynamic simulation considering equilibrium cooling carried out using FACT SAGE 8.1, applying the equilibrium module and the data bases: FSteel and Misc. The selected temperatures were between 400 °C to 1200 °C.

For the microstructural study, samples were mounted in phenolic resin and prepared for the microscopy observation by polishing using SiC papers (320, 400, 600, 800, 1000 and 1200) and diamond paste from 6 μm to 1 μm. The metallographic etchant applied was Nital 2. The optical microscopy observations were performed using a light microscope OLYMPUS GX51 with a LECO IA32 image analysis system. All the phases and microconstituents present in the samples were identified. In addition, microhardness (H_V) measurements were carried out using a LECO LMT 300 instrument with a load of 0,245 N. Finally, the experimental results were correlated with the thermodynamic simulations.

RESULT AND DISCUSSION

Ferritic-bainitic steels (DP-590) present a biphasic structure with different amount of ferrite and bainite, this last microconstituent increases the mechanical properties of the automotive sheet. In consequence, this steel grade improves the overall crash safety of the vehicle. In addition, two other mechanisms are involved to increase the steel final strength: a second phase

hardening (due to bainite formation) and grain refinement phenomena.
DP 590 steel is considered a low carbon steels (C < 0.1 wt.%), with a main purpose to improve formability and weldability.
The relatively high amount of Mn (between 1 and 1.5 wt.%) is added to refine the ferritic grain and prevents the growth of fine carbides, as the eutectoid temperature decreases [10]. Additionally, Si is added to produces equiaxed ferrite grains and to inhibit carbides precipitation into the bainite [10, 11].
From the point of view of mechanical properties behaviour, DP-590 steels have a unique combination of high tensile strength and high hole expansion ratio due to improved stamping ability compared to conventional HSS and DP steels, with the same resistance levels. Another characteristic of the ferritic-bainitic steels is the potential to endure dynamic loads during crash event due to the high energy absorption capacity, while exhibiting good fatigue properties. For this reason, they are suitable for cold-formed automotive components such as profiles, body reinforcements, wheels, and chassis parts, resulting in reduced vehicle weight and higher fuel efficiency [10].
To obtain these types of steels, with specific mechanical properties, it is necessary to carry out a careful control of thermomechanical processing variables, to achieve the adequate phase transformation temperatures and cooling rates.

Thermal characterization by dilatometry tests

Solid state phase transformations in steels during continuous cooling can be studied by dilatometry tests in agreement with several authors [12-20]. Dilatometry is probably the most widely used technique because allows to measure the relative change in length of specimens as function of temperature or time.
The thermal cycle that experiments the sample inside the furnace of the instrument, allows to determine the relative change in the length or thermal strain, defined through the expression (1.):

$$e_{th} = \frac{\Delta L}{L_0} = \frac{L(T) - L_0}{L_0} \qquad (1.)$$

where e_{th} is the relative change in the length or thermal strain, L(T) is the instantaneous length at temperature T and L_0 is the initial length that generally corresponds at room temperature (T_0 = 25 ºC).
By the expression (2.) it is possible to determine the phase transformation temperatures during continuous cooling of steels, since it is a function of temperature:

$$e_{th} = \frac{\Delta L}{L_0} = f(T) \qquad (2.)$$

The test results are plotted in a $\Delta L/L_0$ (%) vs. T (°C) diagram, denominated dilatometric curve. The curve could be done during heating or cooling process.
These curves indicate expansions and contractions experimented by the steel during the thermal treatment.
For this study, the dilatometric curves of all the samples were considered for the cooling conditions.
Fig. 1 shows as an example, the dilatometric curve for DP-590 steel, cooled at the cooling rate 0.45 °C/s.
The steel curve, verifies that the alloy presents a considerable slope variation between 750 °C to 650 °C and indicates the start and finish temperatures of $\gamma \rightarrow \alpha$ phase transformation (which occurs at this temperature range).
The phase transformation is characterized by a variation of the thermal expansion coefficient which is determined by $\Delta L/L_0$ (%) due to the crystalline structure changes produced by allotropy.

At higher temperatures than 750 °C, austenite (or γ solid solution) is the most stable phase in this DP-590 steel. The γ crystalline structure presents Fe atoms at each unit cell corner and in the center of each face of the cube.

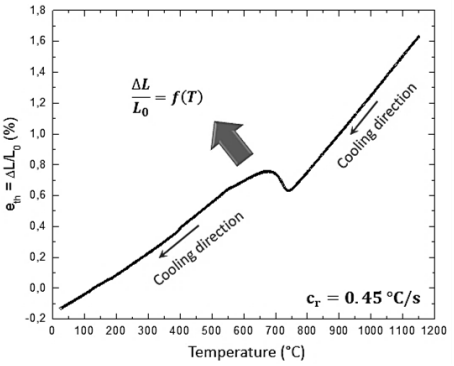

Fig. 1 Dilatometric curve for DP-590 steel obtained at the cooling rate 0.45 °C/s.

In addition, small solute atoms, such as carbon, are placed in interstitial sites. This type of crystalline structure is called face centered cubic (FCC). On the base of primitive cell formalism associated with FCC structure, the atomic volume for the austenite cell is determined by expression (3.):

$$V_\gamma = \frac{a_\gamma^3}{4} \qquad (3.)$$

where V_γ is the austenite unit cell volume and a_γ the austenite unit cell parameter. When $\gamma \rightarrow \alpha$ steel transformation temperature is achieved, the sample experiments a volume change, because the ferrite (BCC) phase starts to nucleate in the austenite (FCC) grain boundaries. The $\gamma \rightarrow \alpha$ phase transformation continuous meanwhile the cooling conditions are favorable. The ferrite (α) phase (BCC) presents a higher unit cell volume fraction respect the (γ) (FCC). In BCC crystalline structure Fe atoms are placed in each corner of the cubic cell and in the center of it. The unit cell volume of α is determined by (4.):

$$V_\alpha = \frac{a_\alpha^3}{2} \qquad (4.)$$

where V_α is the ferrite unit cell volume and a_α is the ferrite unit cell parameter. The impact of the unit cell volume change produced during $\gamma \rightarrow \alpha$ phase transformation is registered by the dilatometric test. In consequence the curve ($\Delta L/L_0$ vs. T) allows to determine the transformation temperature starts and finish through the slope changes.
There are two main methods that allow to determine the critical temperatures of the steel transformation along continuous cooling in a dilatometric curve [21]: a) linear regression and b) first order derivative criterion. **Fig. 2** shows the application of the linear regression method, used in this paper for the mentioned purpose.
It is relevant to comment that the method is described in the ASTM A 1033 standard [22].
This standard is commonly used to provide steels phase transformations data, required for use in numerical models that supply predictions of microstructures, properties, and distortion during the manufacturing process (forging, casting, heat treatment, and welding). In addition, is needed for the construction

of transformation diagrams. The practice covers the steel phase transformation behavior determined through high-speed dilatometry techniques for measuring linear dimensional change as a function of time and temperature.
There are two zones of the dilatometric curve that can be fit with a polynomic of 1° order (Fig. 2):
a) before austenite decomposition, where the thermal dimensional changes are linear and represented by the expression (5.):

$$\frac{\Delta L}{L_0} = A_0 T + B_0 \qquad (5.)$$

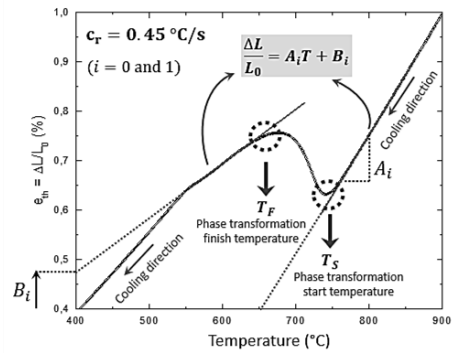

Fig. 2 Dilatometric curve obtained at 0.45 ºC/s cooling rate, showing the critical temperatures of $\gamma \rightarrow \alpha$ phase transformation identified as T_S and T_F.

where A_0 is the selected curve zone slope and B_0 is interception point with y-axis.
b) after austenite decomposition, where the thermal dimensional changes are linear and represented by (6.):

$$\frac{\Delta L}{L_0} = A_1 T + B_1 \qquad (6.)$$

where A_1 and B_1 are the coefficients of the linear function that corresponds to austenite decomposition products.
Based on the described thermal behaviour, a lineal regression was drawn pre and post slope changes on the curve dilatometric, which indicates the $\gamma \rightarrow \alpha$ phase transformation temperature range. The method allows to stablish the $\gamma \rightarrow \alpha$ phase transformation start at T_S = 759 °C and finishes at T_F = 639 °C (Fig. 2).
A similar method was also applied by Pawłowski [23], to determine the phase transformation temperatures during continuous heating, considering various heating rates.
Motycka and Kovér in [24], describe a similar method that consists in draw a straight tangent respect the curve in order to determine the critical points determination, and Vázquez-Gómez et. al [21], explain the linear regression and first derivate alternative method, to determine phase transformation temperatures in steels.
The obtained results allow to consider in the selected dilatometric curve for DP-590 steel at a cooling rate 0.45°C/s, three different fields (**Fig. 3**):

Field I which shows the temperature range of austenite (γ) stability at T ≥ 759 °C for this steel.
Field II indicates the temperatures range of $\gamma \rightarrow \alpha$ phase transformation starts and finish between T = 759 °C to T = 639 °C.
Field III shows the temperatures range in which ferrite phase (α) is stable at T ≤ 639 °C.

It is possible to assume that this plot could be consider as a phases stability field diagram for DP-590 steel, at the selected cooling condition.
Field I is considered the temperatures range at which the (γ) austenite phase (solid solution of C in iron FCC) is stable. The Field II is assumed as the conditions of coexistence between the rich carbon austenite with ferrite. The (α) ferrite phase (solid solution of C in iron BCC) starts to nucleate in the (γ) grain boundaries and growths up to the complete austenite decomposition.
Finally, the Field III, at T ≤ 639 °C, indicates the temperatures range of ferrite (α) stability, after the complete austenite decomposition.
A similar analysis was carried out on the dilatometric curves obtained for all the cooling rates (0.03 °C/s to 100 °C/s). The results provide very useful information of the steel structural evolution at different thermal conditions, and it is considered very useful to design the industrial thermomechanical process conditions for the DP 590 steel.

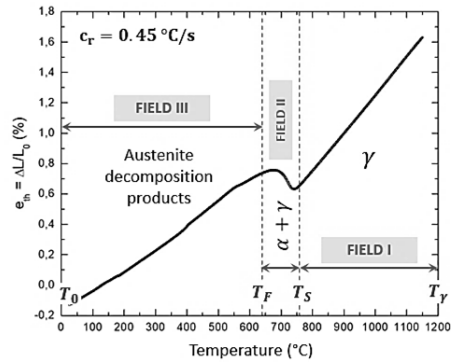

Fig. 3 Fields of phases stability and transformation temperature range determined by a dilatometric curve obtained for the cooling rate 0.45 °C/s.

It is necessary to highlight that the stability of phases and microconstituents strongly depends on the cooling rate with which the heat extraction is carried out in the continuous cooling of the DP-590 steel, because determines the diffusion conditions evolution.
As will be seen later in the paper that was corroborated through optical microscopy, that at low cooling rates, the stable phases in the Field III resulted in a structure of ferrite and pearlite. However, for intermediates cooling rates, the final structure presented ferrite and bainite. Finally, for the highest cooling rates, the structure presents martensite, which constitutes a microconstituent generated without diffusion presence.
The second method used in this study, that allows to obtain the phase transformation temperatures is the dilatometric curve first order derivative criterion, that is $d\Delta L/dt = h(T)$. The first-order derivative of elongation with respect to time is a very useful tool that provides more clarity on the inflection points of the dilatometric curve (observed in Fig. 1), because shows the maximums and minimums at different phases stability fields during continuous cooling of DP-590 steel. **Fig. 4** presents the mentioned $d\Delta L/dt = h(T)$ function corresponding to the cooling rate 0.45 °C/s.
It is possible to consider in **Fig. 4** the same previous three field (I, II and III), associated to phases stability and transformation conditions.

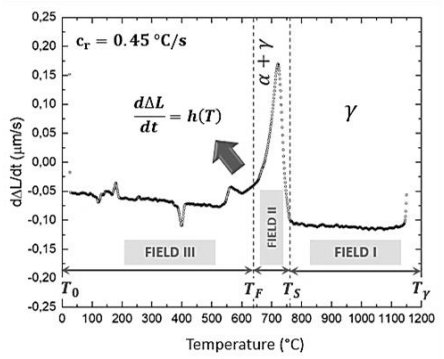

Fig. 4 First order derivative of the dilatometric curve of DP-590 steel, cooled at 0.45 °C/s.

When γ solid solution decomposition is reached, the system undergo expansion due to the contribution of two phenomena that occurs during solid state phase transformations, in steels: a) nucleation and growth of ferrite and b) carbon atoms austenite enrichment. This allows explain why field II (of Fig. 3) experiments expansion between T_F and T_S, during continuous cooling. Furthermore, this behaviour can be corroborated in Fig. 4, due to derivative curve reaches a maximum in field II. **Fig. 5** shows the overlap of both curves (dilatometric curve and derivative curve for the cooling rate 0.45 °C/s.

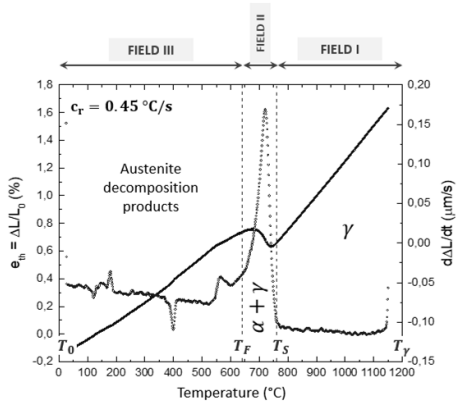

Fig. 5 Overlap of the dilatometric curve and their derivative one, obtained for the cooling rate 0.45 °C/s.

Applying both methods, a linear regression and first order derivative, the critical temperatures for DP-590 steel, were determined for all the cooling conditions considered. In **Table 2**, the $\gamma \rightarrow \alpha$ phase transformation temperatures start, and finish determined for cooling rates between 0.03ºC/s and 100 ºC/s, are presented. It is relevant to comment that the table shows only the main $\gamma \rightarrow \alpha$ phase transformation temperature values obtained in order to evaluate the cooling rate impact.

It is important to observe that the higher the cooling rate is the lower the start and finish transformation temperature $\gamma \rightarrow \alpha$ is.

On the base on all the temperatures obtained the continuous cooling curve (CCT) of DP-590 steel was build.

It is possible to identify certain zones on the steel CCT curve:

austenite (γ) → ferrite (α) + pearlite (P).

austenite (γ) → ferrite (α) + bainite (α_b).

austenite (γ) → ferrite (α) + ferrite (α').

Table 2 DP-590 $\gamma \rightarrow \alpha$ phase transformation temperatures start (T_S) and finish (T_F) determined for cooling rates between 0.03ºC/s and 100 ºC/s.

C_r (°C/s)	T_S (°C)	T_F (°C)	C_r (°C/s)	T_S (°C)	T_F (°C)
0.03	799 ± 1	760 ± 1	2.50	716 ± 1	566 ± 1
0.05	794 ± 0	747 ± 1	3.50	700 ± 1	566 ± 1
2.00	778 ± 1	505 ± 1	100.00	551 ± 0	325 ± 1

At the highest cooling rates, the α' ferrite microconstituent could be constituted by a combination of bainite and martensite or fully martensite.

Fig. 6 shows the CCT curve for DP-590 steel, showing the different microconstituent fields overlapped with the main cooling rates, between (0.03 °C/s to 100 °C/s).

Dash straight lines visualized in the diagram, indicates the theoretical phase transformation temperatures obtained through empirical expressions based on the chemical composition of the selected steel.

It is relevant to correlate the theoretical values of reference with the obtained experimental ones to corroborate the experimental results.

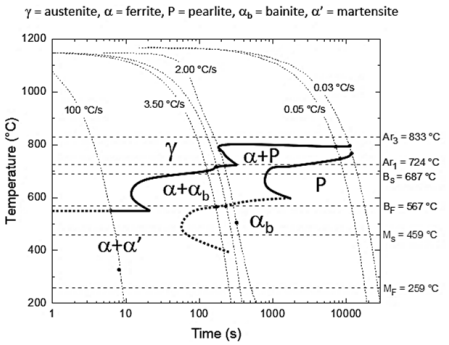

Fig. 6 CCT curve for DP-590 steel indicating the different microconstituent fields.

The theoretical temperature range values, considering start (Ar_3) and finish (Ar_1) of the transformation ($\gamma \rightarrow \alpha$ + P) for DP-590 steel, are given by Lutsenko's equations [25] and determined by (7.) and (8.):

$$Ar_3 = 913{,}70 - 207{,}13\, w_C - 46{,}60\, w_{Mn} + \\ +110{,}54\, w_{Cr} + 108{,}10\, w_N \qquad (7.)$$

$$Ar_1 = 741{,}70 - 7{,}13\, w_C - 14{,}09\, w_{Mn} + \\ +16{,}26\, w_{Si} + 11{,}54\, w_{Cr} - 49{,}69\, w_{Ni} \qquad (8.)$$

In the other hand, the start temperatures of bainite (B_S) and martensite (M_S) formation are given by Bohemen´s equations [26], calculated by (9.) and (10.):

$$B_S = 839 - (86\, w_{Mn} + 23\, w_{Si} + 67\, w_{Cr} + \\ +33 w_{Ni} + 75\, w_{Mo}) - 270[1 \\ - \exp(-1.33\, w_C)] \qquad (9.)$$

$$M_S = 565 - (31\, w_{Mn} + 13\, w_{Si} + 10\, w_{Cr} + \\ +18\, w_{Ni} + 12\, w_{Mo}) - 600[1 \\ - \exp(-0.96\, w_C)] \qquad (10.)$$

The temperatures values of all the expressions are given in centigrade degree (ºC) and the elements weight (w_i) in weight percent.
Continuous cooling transformations diagram is a very important tool that allows to design the industrial thermomechanical processing of the steels. It is not considered as an equilibrium diagram. However, it is a phase diagram which shows the phases present for different cooling rates.
This tool allows to establish that at low cooling rates, between 0.03ºC/s and 0.50ºC/s and in the range between A_{r3} and A_{r1} the atomic diffusion process promotes the austenite solid solution phase transformation to ferrite + pearlite microconstituents, which are stables in the steel microstructure.
If the values of T_S and T_F determined, are between B_S and B_F temperature range, the atomic diffusion process is considerable limited, and the microstructure does not develop microconstituents in a stable equilibrium condition. In this case, the ferrite combined with bainite are formed for these cooling conditions.
At highest cooling rate, when the atomic diffusion process is fully limited, the austenite transformation to ferrite, only results in martensite microconstituent present in the steel microstructure.
It is relevant to mentioned that the industrial processing of DP-590 steel requires a final microstructure with ferrite and 20 % of bainite in order to achieve the mechanical properties adequate for the automotive application. For this reason, it is necessary to corroborate the results through a metallography study.

Microstructural characterization

It is known that the microstructural characteristics such as phases or the present microconstituents, grain size and microhardness values are fundamental to predict the steel sheet finals mechanical properties. For this reason, the characterization of the material in as received state, was considered as good reference information to compare with all the samples heat treated (considering all the cooling rates selected). **Fig. 7** shows the microstructure of DP-590 steel, as received, that corresponds to the material before dilatometry tests.

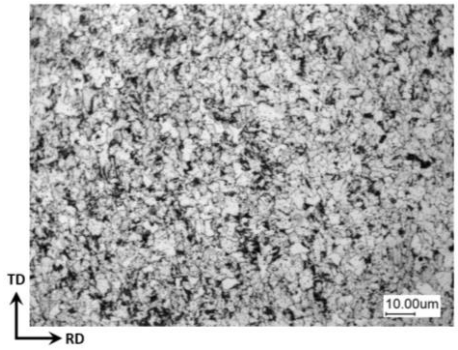

Fig. 7 DP-590 steel as received microstructure aspect.

As can be seen, DP-590 steel presents a microstructure with a very fine grain size. The ASTM grain size number determined was 20, which is equivalent to a grain diameter of 0.32 μm. The microhardness average value is 205 and the specimen presents 80 % of ferrite phase and 20% of bainite.
For this study it is important to determine what could be the adequate cooling rate to achieve the required microstructure and properties characteristics for this steel. This information is useful to adjust the industrial processes variables.

There are two mechanisms that explain the steel transformations: reconstructive and displacive processes [27]. In the reconstructive transformations, the flow of atoms is sufficient to prevent shear stress over crystalline structure of steel. It is important to consider that one of the main product of the austenite reconstructive transformation, is ferrite. α solid solution formation implies the re-arrangement of the iron atoms from the FCC austenite structure to the ferrite BCC structure. In consequence, there is a lattice parameter variation of ferrite. This phenomenon can be described by Vegard's law [28] by (11.):

$$a_\alpha = a_{Fe}^{BCC} + \text{cte}\, x_C \tag{11.}$$

where a_α is the lattice parameter of the α solid solution, a_{Fe}^{BCC} is the lattice parameter of BCC pure Fe and x_C is the C mole fraction. The expression (11.) is possible due to atomic mobility by diffusion that is favored for low thermal extraction at low cooling rates. From energetic point of view, the low cooling rates promotes the diminish of the potential barrier necessary to ferrite nucleation. On the base of γ/γ grain boundary heterogeneous nucleation theory [27], the potential barrier for ferrite nucleation is calculated by (12.):

$$\Delta G^* = \frac{16\pi\sigma_{\alpha\gamma}^3}{3(\Delta G_V + \Delta G_\varepsilon)^2} f(\theta) \tag{12.}$$

where $\sigma_{\alpha\gamma}$ is the ferrite/austenite interfacial energy, ΔG_V is the driving force for $\gamma \rightarrow \alpha$ transformation per unit of volume, ΔG_ε is the strain energy due to crystalline structure change during $\gamma \rightarrow \alpha$ transformation and $f(\theta)$ is a function that depends on the dihedral angle.
It is possible to note that the potential barrier diminishes for high values of ΔG_V and ΔG_ε, and low values of interfacial energy. The mentioned conditions are satisfied for low cooling rates, where equiaxed ferrite grains are formed in steel structure.
Through light microscopy is possible determine that atomic diffusive processes of the specimens cooled at lowest cooling rates, between 0.03 °C/s and 0.50 °C/s, enables the formation of ferrite and pearlite in the DP-590 steel microstructure.
Fig. 8 shows the microstructure obtained in the specimen cooled at 0.03 °C/s, in which the equiaxed (light grey) grains are of ferrite and the black grains are constituted by pearlite. The pearlite microconstituent is formed by lamellar of ferrite and cementite, not resolved at the magnification used in the microscopy observation (100X).

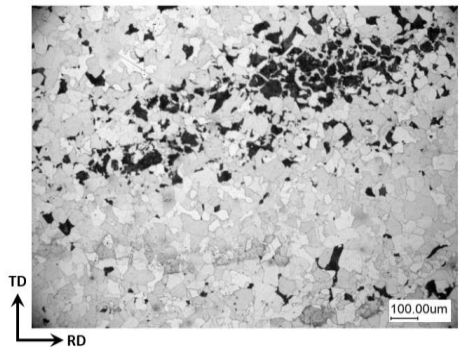

Fig. 8 Microstructure aspect with ferrite and pearlite presence observed in the specimen cooled at 0.03 °C/s.

As result, when samples are cooled between 0.03 °C/s and 0.50 °C/s, the solid-state phase transformation is corroborated by expression (13.):

$$\gamma(T_\gamma, w_C) \rightarrow \alpha(T_S, w_C^\alpha) + P(T_S, w_C^P) \quad (13.)$$

where $\gamma(T_\gamma, w_C)$ is the γ solid solution that is stable at austenitizing temperature T_γ, $\alpha(T_S, w_C^\alpha)$ is the α solid solution that is stable at start temperature and $P(T_S, w_C^P)$ is pearlite. w_C^α and w_C^P indicate the carbon partitioning between ferrite and pearlite, respectively.

According to the cooling rate increases, the atomic diffusive processes are limited. This induces the formation with acicular ferrite morphology microconstituents. For steel DP-590, the second phase formed is bainite. Bhadeshia in [27], comments that during the bainite transformation there is no redistribution of substitutional solutes. However, the mobility of interstitial atoms during bainite formation exists. In this study, it was possible to establish that the bainite is stable for cooling rates between 0.50 and 50 °C/s in the DP-590 steel. **Fig. 9** shows the microstructure observed in the specimen cooled at 3.50 °C/s.

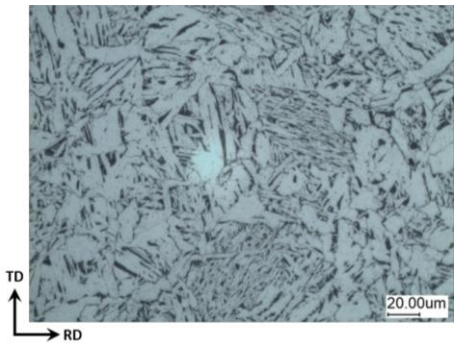

Fig. 9 Bainite observed in the microstructure of the specimen cooled at 3.50 °C/s.

In consequence, it is possible to consider that when the cooling conditions are between 0.50 °C/s and 50 °C/s, the bainite transformation is corroborated in DP-590 microstructure. This transformation could be interpretated through expression (14.).

$$\gamma(T_\gamma, w_C) \rightarrow \alpha(T_S, w_C^\alpha) + \alpha_b(T_S, w_C^{\alpha_b}) \quad (14.)$$

where $\gamma(T_\gamma, w_C)$ is the γ solid solution that is stable at austenitizing temperature T_γ, $\alpha(T_S, w_C^\alpha)$ is the α solid solution that is stable at start temperature and $\alpha_b(T_S, w_C^{\alpha_b})$ is bainite. w_C^α and $w_C^{\alpha_b}$ indicate the carbon partitioning between ferrite and bainite, respectively.

It is well known that one of the strengthening mechanisms of steels is the grain refinement. The relationship between yield strength and grain size commonly used is known as the Hall-Petch equation [27]. This equation shows that a diminish of grain size implies an increment of mechanical resistance of material. It was possible to established for DP-590 steel, that the higher the cooling rates the lower the grain size values. In this study, for the lowest cooling rate (0.03 °C/s), a grain size value of 44.194 μm was obtained, and for cooling rates (10 °C/s) a considerably lower value of grain size was obtained (3.545 μm). For the higher cooling rates carried out, the presence of a fully bainitic or martensitic structure turned complex the grain size determination.

In coincidence with the increase of the bainite volumetric fraction in the steel sample's structure cooled at the faster cooling rates, the mechanical strength increase in the steel specimens also were determined.

The Vickers microhardness (H_V) results obtained for each specimen are consistent with thermal profile applied and structural study. The microhardness average value for the sample treated at a cooling rate 0.03 °C/s was H_V = 127. For the intermediate cooling rate 10 °C/s, the average value obtained was H_V = 230. **Fig. 10** presents the microhardness values distribution in relation with the cooling rates used in the study.

The overlap of the microscopy study results allows to visualize three main fields in the plot:

Ferrite (α) + pearlite (P), for 0.03 °C/s < $\mathbf{c_r}$ < 0.50 °C/s.

Ferrite (α) + bainite (α_b), for 0.50 °C/s < $\mathbf{c_r}$ < 50 °C/s.

Ferrite (α) + martensite (α'), for 50 °C/s < $\mathbf{c_r}$ < 100 °C/s .

The information obtained could be a good control parameter for the automotive steel sheet processing.

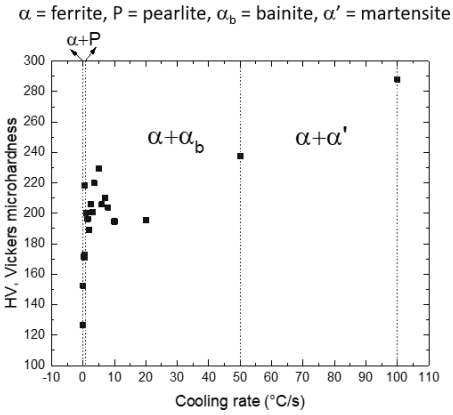

Fig. 10 Vickers microhardness values evolution in relation with cooling rates used in the study. Each point on this graph represents the average of ten Vickers microhardness measurements made in the rolling direction of the steel plate.

Theoretical calculations by Fact Sage

A study of equilibrium conditions on DP-590 steel was carried out by Fact Sage 8.1 software. This software is an important tool that allows to predict thermodynamics properties of materials [8].

The thermodynamic simulation carried out on the base of DP-590 steel chemical composition and the temperature conditions of interest provided all the transformation temperatures, the phases stabilities under equilibrium states.

On this base the optimal parameters for cooling processing were approximated. **Fig. 11** shows the phases stability diagram, built for DP-590 steel at equilibrium conditions. The diagram provides the temperature range of ferrite (α) and austenite (γ) stability together with the percentage (wt. %) of phase in the structure. In addition, the diagram provides information on the evolution of phases percentage in the combined field (γ + α), associated with the transformation temperature range (T_S to T_F).

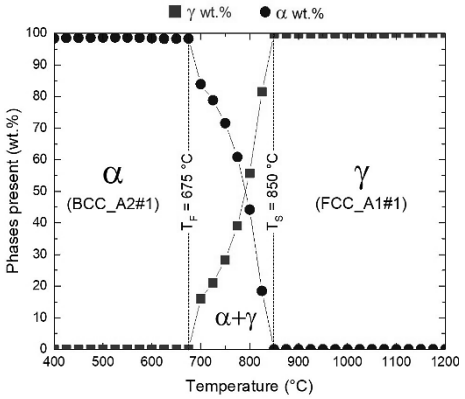

Fig. 11 Stability phase diagram of DP-590 steel, showing the percentage of phases evolution in relation with temperature at equilibrium conditions.

According to this diagram, austenite or γ solid solution, is stable until 850 °C. From this temperature (T_S), the instability of austenite phase induces the ferrite phase nucleation in the boundaries of the austenitic grains. This solid phase transformation finish at T_F = 675 °C. Between both temperatures the austenite phase coexists with the ferrite phase.

Also, at Fig. 11, the crystallographic notation is indicated. This notation form corresponds to German index, called as *Strukturbericht* designation:

Letter A corresponds to crystal types where unit cell is formed by pure elements.

If number is 1, corresponds to FCC structures.

If number is 2, corresponds to BCC structures and so one.

After A1 and A2, the formation of other FCC o BCC structures is indicated.

For this reason, the austenite (γ) structure correspond to A1#1 crystal type and ferrite (α) correspond to A2#1 crystal type.

The phase stability is strongly dependent of Gibbs free energy of the system. If consider that cooling is performed at atmospheric pressure (P = 101.325 kPa) and for a particular temperature, Gibbs free energy is defined by the expression (15.):

$$G = \sum_{i=1}^{k} n_i \mu_i \tag{15.}$$

where n_i is the amount of a particular element present in the chemical composition of steel and μ_i is the chemical potential of the i element in solution. For dilute solutions, chemical potential is $\mu_i = \mu_i^0 + RT \ln x_i$. This manner, the equation (15.) can be expressed as (16.):

$$G = \sum_{i=1}^{k} n_i \left(\mu_i^0 + RT \ln x_i\right) \tag{16.}$$

Therefore, the Gibbs free energy of the system is expressed through equation (17.):

$$G = \sum_{i=1}^{k} \left(n_i \mu_i^0 + n_i RT \ln x_i\right) = \\ = \sum_{i=1}^{k} n_i \mu_i^0 + RT \sum_{i=1}^{k} n_i \ln x_i \tag{17.}$$

where μ_i^0 is the chemical potential of the i pure element and x_i is the molar fraction of i element in solution. If the expression (17.) is divided member to member for total amount of elements present in steel ($n = n_{Fe} + n_C + n_{Mn} + \cdots$), the expression (18.) is obtained:

$$g = \sum_{i=1}^{k} x_i \mu_i^0 + RT \sum_{i=1}^{k} x_i \ln x_i \tag{18.}$$

Due to (18.) only depends on temperature, a linear function of the Gibbs free energy is obtained as it is visualized in **Fig. 12**.

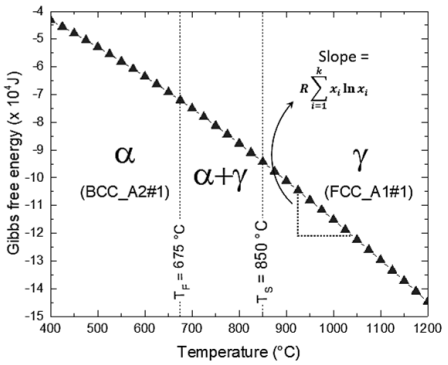

Fig. 12 Gibbs free energy evolution for DP-590 steel at cooling conditions in equilibrium.

Fitting the Gibbs free energy curve, it is possible to obtain (19.):

$$g = 1{,}239.10^4 - 127{,}9.T \tag{19.}$$

This expression (19.) is valid for the temperatures between 400 °C and 1200 °C, at equilibrium cooling conditions. It is easy see that in each temperature range phases stability through Gibbs free energy. For this reason, at higher temperatures γ solid solution is stable. According to dilatometric curves, austenite is the most stable phase of DP-590 steel at elevate temperatures. In the other hand, for temperatures minor that T_F = 675 °C, α solid solution is the stable phase at lower temperatures. Fact Sage simulations are made in equilibrium cooling conditions. However, since the dilatometric curves correspond to non-equilibrium cooling conditions, the latter show that the ferrite is also stable below T_F. For high cooling rates, the ferrite is stable in the form of bainite.

Finally, the evolution of precipitates at equilibrium cooling conditions with temperature was studied. Due to Nb and Ti are in the DP-590 steel, it is probably that niobium carbide (NbC) and titanium carbide (TiC) can be formed. **Fig. 13** shows the evolution of the total amount of precipitates, expressed in weight percent and the total amount of precipitates should be understood as the combination of NbC + TiC. **Fig. 14** shows an image of a titanium carbide particle observed and analyzed by EDS at sample corresponding to a cooling rate of 2 °C/s.

As can be seen, the volume fraction of precipitates increases as the temperature decreases.

In other words, as heat is removed from the system, the total amount of precipitates increases. However, before the decomposition of the austenite, the volume fraction of precipitates is stabilized at a value around 6.60 10^{-2} wt. %.

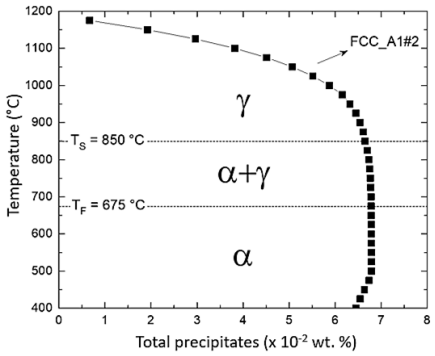

Fig. 13 Evolution of mass fraction of total precipitates in equilibrium cooling conditions.

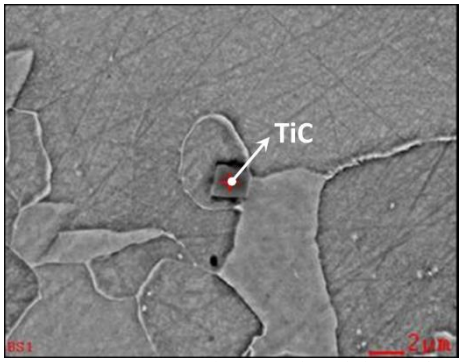

Fig. 14 Titanium carbide (TiC) at sample cooled at 2 °C/s.

According to Bhadeshia in [29], these compounds formation contribute to the steel strengthening mechanism through precipitation. By this way, the improvement of the final mechanical properties of the steel product is achieved.

CONCLUSIONS

Ferritic-Bainitic (FB) steels are very important materials for automotive applications. The results obtained on DP590 steel allows to say that dilatometry tests constitute a convincing technique to provide useful information associated with solid state phase transformation in the steels. By this methodology it was possible to determine the $\gamma \rightarrow \alpha$ phase transformation temperatures of start and finish (T_S and T_F), for all the cooling rates considered in the study. These temperatures are very important variables for DP-590 processing. For lower cooling rate considered in this study (0.03 °C/s) T_S = 799 °C and T_F = 760 °C, and for an intermediate cooling rate (3.50 °C/s), T_S = 700 °C and T_F = 566 °C.

The correlation of the dilatometry results with the microstructural study including values of microhardness, allowed to define the continuous cooling diagram and the microconstituent stability fields for DP-590 steel, considering cooling rates between 0.03ºC/s to 100ºC/s. The CCT curves built constitutes a relevant phase diagram to design thermomechanical processing of DP-590 steel, in the steel industry. For lower cooling rate considered in this study (0.03 °C/s), the final microstructure is formed by ferrite and perlite. In the other hand, for an intermediate cooling rate (3.50 °C/s), the final microstructure is formed by ferrite and bainite.

Through the microstructural study it was possible determine at which cooling rates the combination of ferrite and bainite start to be formed in the structure of DP590 steel. In addition, which is the required cooling rate to obtain the 20% of bainite and 80% of ferrite proportion in the DP590 steel microstructure. This microconstituents proportions are necessary to achieve the mechanical behaviour for the automotive steel parts production by stamping.

Grain refinement mechanism together with microconstituents combination enhanced the mechanical strength according to the stamping requirements of the steel, as was corroborated by microhardness measurements.

By Fact Sage it was possible to corroborate the phase transformation temperatures and to predict the precipitation phenomena evolution in the steel during cooling. Niobium and titanium carbides were determined as possible stable precipitates that could be formed during DP590 steel cooling, by the software.

This information is considered a contribution for the industry in which this type of ferritic-bainitic dual-phase steels is produced. It is relevant to highlight that the information obtained allows to adjust industrial thermomechanical processes variables for this type of steel grades.

Acknowledgments: The authors wish to thank the Universidad Tecnológica Nacional for providing financial support to carry out this research.

REFERENCES

1. M. Tisza, I. Czinege: International Journal of Lightweight Materials and Manufacture, 1, 4, 2018, 229-238, https://doi.org/10.1016/j.ijlmm.2018.09.001.
2. C.D. Horvath: Advanced steels for lightweight automotive structures, *Materials, Design and Manufacturing for Lightweight Vehicles*, Cambridge: Woodhead Publishing Limited, 2021, 39-95, https://doi.org/10.1016/B978-0-12-818712-8.00002-1.
3. T.A. Kop, J. Sietsma, S. Van Der Zwaag: Journal of Materials Science, 36, 2001, 519-526, https://doi.org/10.1023/A:1004805402404.
4. C. Capdevila, F. G. Caballero, C. García De Andrés: Metallurgical and Materials Transactions A, 32, 2001, 661-669, https://doi.org/10.1007/s11661-001-1001-1.
5. M. Gómez, S.F. Medina, G. Caurana: ISIJ International, 43, 8, 2003, 1228-1237, https://doi.org/10.2355/isijinternational.43.1228.
6. S. Choi: Materials Science and Engineering A, 363, 1, 2003, 72–80, https://doi.org/10.1016/S0921-5093(03)00587-2.
7. D. San Martin, P.E.J. Rivera Diaz del Castillo, C. García De Andrés: Scripta Materialia, 58, 10, 2008, 926-929, https://doi.org/10.1016/j.scriptamat.2008.01.019.
8. E. Brandaleze, M. Romanyuk: Acta Metallurgica Slovaca, 28, 2, 2022, 71–79, https://doi.org/10.36547/ams.28.2.1416.
9. H. K. D. H. Bhadeshia: Bainite in Steels, 3rd edition, Leeds: Maney Publishing, 2015.
10. M. Cai, H. Di: Advanced high strength steels and their properties, *Rolling of advanced high strength steels: Theory, simulation, and practice*, eds. J. Zhao and Z. Jiang, Boca Raton: CRC Press - Taylor & Francis Group, 2017, 1-25.
11. M. Cai, H. Ding, Y. Lee, Z. Tang, J. Zhang: ISIJ International, 51, 3, 2011, 476-481, https://doi.org/10.2355/isijinternational.51.476.
12. M. Takahashi, H. K. D. H. Bhadeshia: Journal of Materials Science Letters, 8, 1989, 477-478, https://doi.org/10.1007/BF00720712.

13. C. García de Andrés, F. G. Caballero, C. Capdevila, H. K. D. H. Bhadeshia: Scripta Materialia, 39, 6, 1998, 791-796, https://doi.org/10.1016/S1359-6462(98)00146-8.
14. J. D James, J. A. Spittle, S. G. R. Brown, R. W. Evans: Measurement Science and Technology, 12, 3, 2001, R1-R15,
15. F. G. Caballero, C. Capdevila, C. García de Andrés: ISIJ International, 41, 10, 2001, 1039-1102, https://doi.org/10.2355/isijinternational.41.1093.
16. R. A. Jaramillo, M. T. Lusk, M. C. Mataya: Acta Materialia, 52, 4, 2004, 851-858, https://doi.org/10.1016/j.actamat.2003.11.017.
17. J. Y. Kang, S. J. Park, D. W. Suh, H. N. Half: Materials characterization, 84, 2013, 205-215, https://doi.org/10.1016/j.matchar.2013.08.002.
18. S. Salari, M. Naderi, U. Prahl, and W. Bleck: Advanced Materials Research, 622-623, 2013, 581-584, https://doi.org/10.4028/www.scientific.net/amr.622-623.581.
19. Z. Jiang, C. Deng-Fu, Z. Cheng-Qian, H. Weng-Sing, H. Ming-Rong: Journal of Materials Research, 30, 13, 2015, 2081-2089, https://doi.org/10.1557/jmr.2015.173.
20. Y. Xu, G. Xu, X. Mao, G. Zhao, S. Bao: Metals, 7, 9, 2017, 1-13, https://doi.org/10.3390/met7090330.
21. O. Vázquez-Gómez, A. I. Gallegos-Pérez, E. López-Martínez, H. J. Vergara-Hernández, J. A. Barrera-Godinez: Journal of Thermal Analysis and Calorimetry, 135,6, 2019, 2985-2993, https://doi.org/10.1007/s10973-018-7449-7.
22. ASTM A 1033: Standard practice for quantitative measurement and reporting of hypoeutectoid carbon and low-alloy steel phase transformations. West Conshohocken: ASM International, 2004.
23. B. Pawłowski: Journal of Achievements in Materials and Manufacturing Engineering, 54, 2, 2012, 185-193.
24. P. Motycka, M. Kovér: Evaluation methods of dilatometer curves of phase transformations. COMAT 2012: 2nd International conference on recent trends in structural materials, The Czech Republic, 2012.
25. A. A. Gorni: *Steel forming and heat-treating handbook*, 2019, http://www.gorni.eng.br/e/Gorni_SFHTHandbook.pdf.
26. S. M. C. Van Bohemen: Materials Science and Technology, 28, 4, 2012, 487-495, https://doi.org/10.1179/1743284711Y.0000000097.
27. H. K. D. H. Bhadeshia, R. W. K. Honeycombe: Steels: Microstructure and Properties, 4th Edition, Oxford: Butterworth-Heinemann, 2017.
28. E. J. Mittemeijer: Fundamentals of Materials Science, Heidelberg: Springer, 2010.
29. H. K. D. H. Bhadeshia: *Theory of Transformations in Steels*, 1st Edition, Boca Raton (FL): CRC Press, 2021.